JOURNAL OF NANO- AND ELECTRONIC PHYSICS
Vol. 9 No 6, 06007(6pp) (2017)

ЖУРНАЛ НАНО- ТА ЕЛЕКТРОННОЇ ФІЗИКИ
Том 9 № 6, 06007(6cc) (2017)

# Electron Scattering on the Short-range Potential of the Point Defects in Sphalerite GaN: Calculation from the First Principles

O.P. Malyk*, S.V. Syrotyuk

*Lviv Polytechnic National University, Semiconductor Electronics Department, 12, S. Bandera Str., 79013 Lviv, Ukraine*

(Received 20 May 2017; revised manuscript received 15 November 2017; published online 24 November 2017)

The electron scattering processes in sphalerite gallium nitride on the different lattice point defects are considered. The short-range principle is taken into account in all the calculations. The transition matrix elements have been evaluated by using the self-consistent wave function and potential obtained within the *ab initio* density functional theory. This approach avoids the problem of using the fitting parameters for the six electron scattering mechanisms. The temperature dependences of electron mobility in the range 30-300 K are calculated. The results obtained with short-range scattering models reveal a better agreement with experiment than with the long-range scattering ones. For the first time the electron transport properties have been obtained here on base of the short-range scattering models, with derived by projector augmented waves self-consistent eigenfunctions and potentials, calculated from the first principles.

**Keywords**: Electron transport, Point defects, DFT calculation.

DOI: 10.21272/jnep.9(6).06007 PACS number: 72.20.Dp

## 1. INTRODUCTION

Usually the description of the charge carrier scattering process on the point lattice defects in II-VI and III-V compounds was carried out by relaxation time approximation, variational method and Monte Carlo approach. The common feature of these methods is the using of the long-range charge carrier scattering models for the description of the transport phenomena in these semiconductors. On the other hand in the series of papers [1, 2] it was shown the disadvantages of these models and it was proposed a new approach for description of the transport phenomena on the base of the short-range principle. However in the proposed approach the one disadvantage remains, namely the presence of some numerical fitting parameters which require the availability of experimental data to select their numerical values. At present paper a new method is proposed that enables to eliminate the majority of the fitting parameters. In this method the calculation of the charge carrier transition probabilities was carried out on the base of wave function and self-consistent potential which were determined from the first principles using the projector augmented waves (PAW), as implemented in the ABINIT code [3].

## 2. CALCULATION OF THE ELECTRON WAVE FUNCTION

Calculation of the kinetic coefficients in a crystal is based on the transition matrix elements. The latter are evaluated on the all-electron wave functions. Therefore, the all-electron eigenfunctions found on base of the PAW are appropriate for this purpose.

The PAW approach has been suggested by Blöchl [4]. In the PAW formalism all-electron wavefunction $\Psi_{n\mathbf{k}}$ is defined as a linear transformation from a smooth pesudo-wave function $\tilde{\Psi}_{n\mathbf{k}}$ via

$$\Psi_{n\mathbf{k}}(\mathbf{r}) = \tilde{\Psi}_{n\mathbf{k}}(\mathbf{r}) + \sum_{a,i} < \tilde{p}_i^a | \tilde{\Psi}_{n\mathbf{k}} > \left[\phi_i^a(\mathbf{r}-\mathbf{R}_a) - \tilde{\phi}_i^a(\mathbf{r}-\mathbf{R}_a)\right] \quad (1)$$

The transformation is chosen in such a way that the all-electron wavefunction $\Psi_{n\mathbf{k}}$ is the sum of the pseudo one $\tilde{\Psi}_{n\mathbf{k}}$ and an additive contribution centered on each atom [4]. The electron density is given by equation

$$n(r) = \sum_n f_n \left|\tilde{\Psi}_n(\mathbf{r})\right|^2 + \sum_{a,ij} \rho_{ij}^a \left(\phi_i(\mathbf{r})\phi_j(\mathbf{r}) - \tilde{\phi}_i(\mathbf{r})\tilde{\phi}_j(\mathbf{r})\right), \quad (2)$$

where $f_n$ and $\rho_{ij}^a$ are the occupation number and occupation matrix.

In the augmentation regions, i.e. inside the spheres centered on each atom, the three type of functions are defined: (1) the all-electron basis function $\phi_i^a(\mathbf{r}-\mathbf{R}_a)$, (2) the smoth pseudo-function $\tilde{\phi}_i^a(\mathbf{r}-\mathbf{R}_a)$, (3) the projector function $\tilde{p}_i^a(\mathbf{r})$. Here $\mathbf{R}_a$ denotes the center of augmentation spheres and $n$ enumerates the quantum numbers. The wave vector $\mathbf{k}$ is confined to the first Brillouin zone. The basis functions are defined by the following condition:

$$\tilde{\phi}_i^a(\mathbf{r}) = \phi_i^a(\mathbf{r}), \mathbf{r} > \mathbf{r}_c, \quad (3)$$

i.e. they are matching outside the augmentation sphere of radius $r_c$. The projector functions vanish outside the augmentation sphere and inside the latter they are

* omalyk@ukr.net

 © 2017 Sumy State University

orthogonal to pseudo-functions:

$$< \widetilde{p}_i^a \mid \widetilde{\phi}_i^a > . \quad (4)$$

The all-electron expectation value for any operator $A$ can now be written as

$$< \Psi_{n\mathbf{k}} \mid A \mid \Psi_{n\mathbf{k}} > = < \widetilde{\Psi}_{n\mathbf{k}} \mid A \mid \widetilde{\Psi}_{n\mathbf{k}} > + \sum_{a,ij} < \widetilde{\Psi}_{n\mathbf{k}} \mid \widetilde{p}_i^a > \times < \widetilde{p}_i^a \mid \widetilde{\Psi}_{n\mathbf{k}} > \left[ < \phi_i^a \mid A \mid \phi_i^a > - < \phi_i^a \mid A \mid \phi_i^a > \right]. \quad (5)$$

The eigenfunctions needed in equation (5) can be evaluated from the Schrödinger equation:

$$H \mid \Psi_{n\mathbf{k}} > = E_{n\mathbf{k}} \mid \Psi_{n\mathbf{k}} > , \quad (6)$$

where $H$ is the Hamiltonian operator, $\Psi_{n\mathbf{k}}$ is the eigenfunction, $E_{n\mathbf{k}}$ is the energy eigenvalue. From (1) we can obtain the equation

$$\Psi_{n\mathbf{k}}(\mathbf{r}) = \left( 1 + \sum_{a,i} \left( \mid \phi_i^a(\mathbf{r}) > - \mid \widetilde{\phi}_i^a(\mathbf{r}) > \right) < \widetilde{p}_i^a \mid \right) \mid \widetilde{\Psi}_{n\mathbf{k}} > . \quad (7)$$

Introducing the operator

$$\tau = 1 + \sum_{a,i} \left( \mid \phi_i^a(\mathbf{r}) > - \mid \widetilde{\phi}_i^a(\mathbf{r}) > \right) < \widetilde{p}_i^a \mid \quad (8)$$

we obtain the equation connecting the true all-electron function and pseudowave one:

$$\Psi_{n\mathbf{k}}(\mathbf{r}) = \tau \, \widetilde{\Psi}_{n\mathbf{k}}(\mathbf{r}). \quad (9)$$

Now the definition (9) is substituted into (6), and the eigenvalue problem is reformulated as follows:

$$\tau^+ H \tau \mid \widetilde{\Psi}_{n\mathbf{k}} > = \tau^+ \tau \mid \widetilde{\Psi}_{n\mathbf{k}} > E_{n\mathbf{k}} , \quad (10)$$

where $\tau^+$ is the Hermitian conjugate operator for the transformation $\tau$. Comparison the linear system of equations (10) and Schrödinger equation (6) shows that transformation (9) conserves the electron energy band spectrum $E_{n\mathbf{k}}$

Calculating pseudo-functions $\widetilde{\Psi}_{n\mathbf{k}}$ from equations (10) we find then true wave functions $\Psi_{n\mathbf{k}}$ from equation (9) needed for evaluating the transition matrix elements. The transformation operator $\tau$ (8) is defined on the basis functions $\phi_i^a$ , $\widetilde{\phi}_i^a$ and $\widetilde{p}_i^a$ that are calculated by means of the AtomPAW code [5,6]. The PAW basis functions have been generated for the following valence states: $3s^2 3p^6 4s^2 4p^1 3d^{10}$ for Ga and $2s^2 2p^3$ for N. The radii of the augmentation spheres $r_c$ have the following values: 1.8 and 1. a.u. for Ga and N, respectively. The exchange and correlation effects have been taken into account within the generalized gradient approximation (GGA) formalism suggested by Perdew, Burke and Ernzerhof (PBE) [7], particularly in the form of hybrid PBE functional with Hartree-Fock exchange, PBE0 [8]. The program AtomPAW provides the full set of data that are input parameters for the ABINIT code [3, 9] initialization.

The wave functions and electron energies of the GaN crystal have been obtained by means of the ABINIT code. The experimental value of the lattice parameter $a_0$ = 4.5 Å was used in the calculation. The number of the plane waves for the pseudowave function $\widetilde{\Psi}_{n\mathbf{k}}$ expansion was defined by the maximum value of energy $E_{cut}$ = 64 Ry. The electronic density and crystal Coulomb potential were calculated on the more dense grid defined by limiting energy 128 Ry. Integration over the Brillouin zone was carried out on the Monkhorst-Pack 8 × 8 × 8 grid [10].

## 3. SHORT-RANGE SCATTERING MODELS

In the electron-polar optical phonon short-range scattering model the potential energy of the electron-polar optical phonon interaction has spherical symmetry [1]. The wave function of the system “electron + phonons” was chosen in the form:

$$\Psi = \varphi(\mathbf{r}) \Phi(x_1, x_2 .. x_n) , \quad (11)$$

where $\Phi(x_1, x_1 .. x_n)$ – wave function of the system of independent harmonic oscillators; $\varphi(\mathbf{r})$–electron wave function at the $\Gamma$ point of the Brillouin zone which was obtained from the ABINIT code [7, 13]. After that on the base of the method described in [1] the expression for the transition probability can be defined:

$$W(\mathbf{k},\mathbf{k}') = \frac{\pi^5 A_{PO}^2 e^4}{16 \varepsilon_0^2 a_0^8 G} \frac{M_{Ga} + M_N}{M_{Ga} M_N} \times \left\{ \frac{1}{\omega_{LO}} \left[ N_{LO} \delta(E' - E - \hbar\omega_{LO}) + (N_{LO} + 1) \times \delta(E' - E + \hbar\omega_{LO}) \right] + \frac{2}{\omega_{TO}} \left[ N_{TO} \delta(E' - E - \hbar\omega_{TO}) + (N_{TO} + 1) \delta(E' - E + \hbar\omega_{LO}) \right] \right\}, \quad (12)$$

where $G$ – a number of unit cells in a crystal volume; $M_{Ga}$ , $M_N$ – atomic masses; $N_{LO}$; $N_{TO}$ – the number of longitudinal (LO) and transverse (TO) phonons with a frequency $\omega_{LO}$ and $\omega_{TO}$ respectively; $\varepsilon_0$ – dielectric constant and such notation is introduced:

$$A_{PO} = \int_\Omega \varphi^* (R^2 - \frac{r^2}{3}) \, \varphi \, d\mathbf{r} . \quad (13)$$

The integral $A_{PO}$ over the volume of the unit cell is divided into several parts each of which were calculated on the base of Simpson method by breaking the integration intervals into 44 parts. The calculation of the values of coordinates and function $\varphi^* \varphi$ in the knots of Simpson method was made using the transformations from polar coordinate system to the oblique coordinate system. The values of the function $\varphi^* \varphi$ at respective points in the oblique coordinate system were obtained using the ABINIT code. On the base of three-dimensional B-spline interpolation [11] the values of the function $\varphi^* \varphi$ at the points corresponding to the knots of Simpson method can be calculated. The func-

tion $\varphi^*\varphi$ is a scalar therefore its values in the oblique coordinate system can be put into compliance to the values in the knots of Simpson method in the initial polar coordinate system. Using such approach the value of the integral (13) can be obtained: $A_{PO} = 14.59\times10^{-20} m^2$.

According to short-range scattering model of the electron-nonpolar optical phonon interaction in sphalerite semiconductor the transition probability looks like [1]:

$$W(\mathbf{k},\mathbf{k}') = \frac{\pi^3 d_0^2}{1152\ a_0^2\ G}\ \frac{M_{Ga}+M_N}{M_{Ga}\ M_N}\times \left\{\frac{1}{\omega_{LO}}\left[N_{LO}\delta(E'-E-\hbar\omega_{LO})+(N_{LO}+1)\times \delta(E'-E+\hbar\omega_{LO})\right]+\frac{2}{\omega_{TO}}\left[N_{TO}\delta(E'-E-\hbar\omega_{TO})+(N_{TO}+1)\delta(E'-E+\hbar\omega_{LO})\right]\right\}, \quad (14)$$

where $d_0 = 1.31$ eV– the optical deformation potential constant

The value $d_0$ was calculated on the base of three-dimensional B-spline interpolation [11] and taking into account the longitudinal and the transverse branches of the optical vibrations

From the short-range scattering model of the electron- acoustic phonon interaction in sphalerite semiconductor [2] one can obtain the expression for electron transition probability in a form:

$$W(\mathbf{k},\mathbf{k}') = \frac{\pi^3 k_B T\, E_{AC}^2}{576\,\hbar\, G\,(M_{Ga}+M_N)}\left(\frac{1}{c_{||}}+\frac{1}{c_{\perp}}\right)^2 \delta(E'-E) \quad (15)$$

where $E_{AC}$ – the acoustic deformation potential constant; $c_{||}$ and $c_{\perp}$ – the longitudinal and transverse sound velocity respectively and the elastic character of scattering is taken into account.

The value $E_{AC}$ was calculated on the base of three-dimensional B-spline interpolation [11] and equal $E_{AC} = 0.218\,\text{eV}$.

In the frameworks of the short-range scattering model the potential energy of the electron- piezoelectric phonon interaction has spherical symmetry [1]. As the coordinate dependence of the perturbation energy is similar to a case of PO –scattering therefore the integration over the unit cell is carried out by the method described for this case. This yield to $A_{PZ} = A_{PO} = 14.59 \times 10^{-20}\text{m}^2$. Then using the procedure described in [1] we obtained the transition probabilities for the electron scattering on piezoacoustic (PAC) and piezooptic (POP) phonons:

$$W_{PAC}(\mathbf{k},\mathbf{k}') = \frac{\pi^5 e^2 \mathrm{e}_{14}^2\ A_{PZ}^2\ k_B T}{128\,\hbar\,\mathrm{G}\,\varepsilon_0^2 \mathrm{a}_0^2\,[M_{Ga}+M_N]}\times \left(\frac{1}{c_{||}}+\frac{2}{c_{\perp}}\right)^2 \delta(E'-E); \quad (16)$$

$$W_{POP}(\mathbf{k},\mathbf{k}') = \frac{\pi^7 e^2 e_{14}^2 A_{PZ}^2}{400\ \varepsilon_0^2 a_0^4\ G}\ \frac{M_{Ga}+M_N}{M_{Ga}\ M_N}\times \left\{\frac{1}{\omega_{LO}}\left[N_{LO}\delta(E'-E-\hbar\omega_{LO})+(N_{LO}+1)\times \delta(E'-E+\hbar\omega_{LO})\right]+\frac{2}{\omega_{TO}}\left[N_{TO}\delta(E'-E-\hbar\omega_{TO})+(N_{TO}+1)\delta(E'-E+\hbar\omega_{LO})\right]\right\}. \quad (17)$$

In the frameworks of the short-range scattering model the potential energy of the electron- ionized impurity interaction is spherically symmetric [1]. Therefore the calculation of the transition probability can be done by the method similar for the case of PO-scattering. As a result the transition probability for this scattering mechanism looks like:

$$W(\mathbf{k},\mathbf{k}') = \frac{Z_i^2 e^4 N_{II}\ A_{II}^2\ a_0^6}{512\,\varepsilon_0^2\,\hbar\, V}\,\delta(E'-E), \quad (18)$$

where $N_{II}$ – the concentration of ionized impurities; $A_{II} = 0.693\times10^{-10} m^{-1}$; $Z_i$ – the multiplicity ionization of impurity.

The transition probability for electron interaction with the short-range potential of static strain centre was calculated by one of the authors in [2] and looks like:

$$W(\mathbf{k},\mathbf{k}') = \frac{2^5 3^4 \pi^3 C^2 a_0^6 e^2\ e_{14}^2 N_{SS}}{V\varepsilon_0^2\hbar}\,\frac{1}{q^2}\,\delta(E'-E), \quad (19)$$

where $C \approx 0.1$; $N_{SS}$ – concentration of the static strain centers. In (19) $\mathrm{N_{SS}}$ is the only one adjustable parameter which is remained. However up to our knowledge the method of calculation the value of the concentration of the static strain centers remain unknown.

## 4. COMPARISON OF THEORY AND EXPERIMENT

The comparison of theoretical calculation was made with experimental data presented in [12] for zinc blende GaN epilayers. Four samples were examined: unintentionally doped sample (sample A), intentionally doped samples 1, 3, 5 (samples B, C, D respectively). It was assumed that impurity conductivity occurs due to ionization of the donor impurity. Calculation of Fermi level was held from the expression $n = n_{exp} = 1/R_{exp}$, $R_{exp}$ – experimental value of Hall coefficient. Parameters of GaN used in calculation are presented in Table I. The theoretical and experimental temperature dependences of the electron mobility $\mu(T)$ are presented on Fig. 2a-d. Solid curve 1 was obtained on the base of the short-range scattering models within the framework of the exact solution of the Boltzmann kinetic equation [23] The adjustable parameter $N_{SS}$ for these curves has next numerical value: sample A – $N_{SS} = 1.6\times10^{14}\ \text{cm}^{-3}$; sample B – $N_{SS} = 4.0\times10^{14}\ \text{cm}^{-3}$; sample C – $N_{SS} = 3.0\times10^{15}\ \text{cm}^{-3}$; sample D – $N_{SS} = 3.5\times10^{16}\ \text{cm}^{-3}$. Dashed curves 2 and 3 were calculated on the base of the long-range scattering models within the framework of relaxation time approximation: curve 2 corresponds

**Table 1** – Parameters of GaN (sphalerite) used in calculations

| Material parameter | Value |
|---|---|
| Lattice constant, $a_0$ (m) | $4.5\times10^{-10}$ |
| Energy gap, $E_g$ | $3.299\text{-}5.93\times10^{-4}\,T^2/(T+600)$ [a, b, c] |
| Energy equivalent of the matrix element, $E_p$ (eV) | 25 [a, d, e] |
| Spin-orbit splitting, $\Delta$, (eV) | 0.017 [b] |
| Density, $\rho_0$ (kg m$^{-3}$) | $6.15\times10^3$ [f, g] |
| Optical deformation potential, $d_0$ (eV) | 1.31 [h] |
| Acoustic deformation potential, $E_{AC}$ (eV) | 0.218 [h] |
| Transverse optical phonon frequency, $\omega_{TO}$ (rad s$^{-1}$) | $1.045\times10^{14}$ [i] |
| Longitudinal optical phonon frequency, $\omega_{LO}$ (rad s$^{-1}$) | $1.398\times10^{14}$ [i] |
| Elastic constants ($\times10^{-10}$, N·m$^{-2}$): | |
| $C_{11}$ | 29.3 [j] |
| $C_{12}$ | 15.9 [j] |
| $C_{44}$ | 15.5 [j] |
| Piezoelectric tensor component, $e_{14}$ (C·m$^{-2}$) | 0.4 [k] |

[a] – [13]; [b] – [14]; [c] – [15]; [d] – [16]; [e] – [17]; [f] – [18]; [g] – [19]; [h] Present article; [i] – [20]; [j] – [21]; [k] – [22].

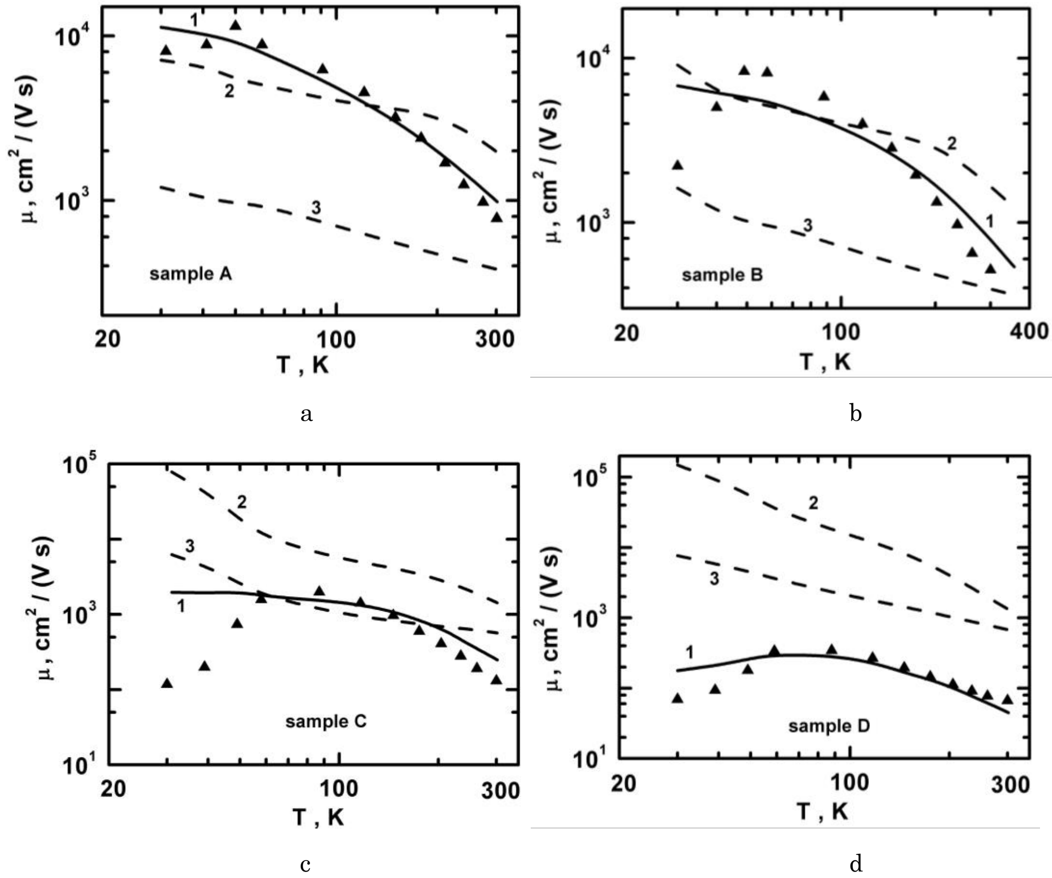


**Fig. 1** – The temperature dependences of electron mobility in $n$-GaN (sphalerite). 1 – short-range scattering models; 2, 3 –long-range scattering models (relaxation time approximation)

to the case of low temperatures $(\hbar\omega >> k_B T)$ whereas curve 3 corresponds to the case of high temperatures $(\hbar\omega << k_B T)$. Comparison of theoretical curves obtained in the two approaches with experimental data shows that the short-range scattering models demonstrate much better qualitative and quantitative agreement with experiment compared with long-range scattering models. This indicates that the short-range models more adequately describe the charge carrier scattering processes than the long-range models. To estimate the role of the different scattering mechanisms on Fig. 3a-b the dashed curves represent the corresponding mobility for the samples with minimum and maximum value of defect concentration. It is seen that at low temperatures the main scattering mechanisms are the static strain scattering (curve 7) and piezoacoustic scattering (curve 4). For the sample with maximum impurity concentration the ionized-impurity scattering (curve 2) plays a prominent role too at this tempera-

ture interval. At high temperature region the piezo-acoustic scattering play the main role. However, at this temperature range the polar optical phonon scattering (curve 5) plays the significant role too and it is probable that at T > 300 K this scattering mechanism becomes dominant. Other scattering mechanisms – AC-, NPO-, POP- scattering mechanisms – give negligibly small contributions.

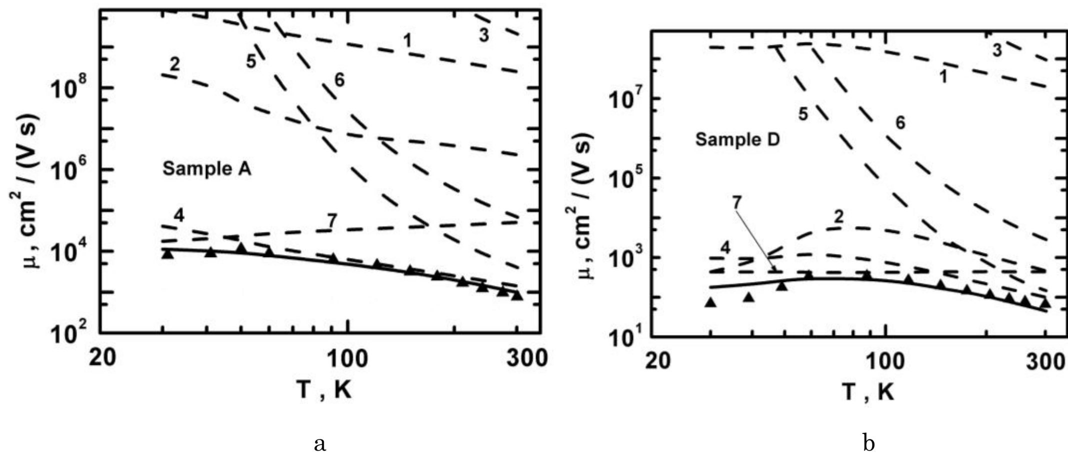


a b

**Fig. 3.** – The contribution of different scattering modes into electron mobility in n-GaN. Solid line - mixed scattering mechanism; 1,2,3,4,5,6,7 – AC-, II-, NPO-, PAC-, PO-, POP-, SS- scattering mechanism respectively

## 5. CONCLUSION

Using the short-range principle the electron scattering processes on the various types of crystal defects in n-GaN are considered. The calculation of the electron transition probabilities was made using the all-electron wave function and a crystal potential, evaluated within the projector augmented waves. The GGA formalism has been used, and the self-interaction effects of Ga 3 d electrons were taken into account in the form of PBE0, as implemented in the ABINIT code. The use of exchange-correlation potential in the form PBE0 allowed getting the value of the band gap close to the experimentally measured value. It is very important for evaluation of realistic matrix elements needed to calculate the kinetic coefficients. We see two components of the success of the theory developed in this paper. The first one covers the realistic self-consistent electronic energy band structure, including the band gap, the all-electron wave functions and crystalline potential GaN, enabled us for the first time to get a good comparison of the theoretical and experimental kinetic coefficients over a wide temperature range. And the second one includes the short-range models of the electron scattering processes. It was found that the results obtained within the short-range models are in much better agreement with the experimental values, than those calculated on base of the long-range models. As can be seen from Figures 2-3 we find nearly perfect agreement between theory and experiment.

# Рассеяние электронов на близкодействующем потенциале точечных дефектов в GaN со структурой сфалерит: расчет из первых принципов

О.П. Малык, С.В. Сыротюк

*Национальный университет «Львовская политехника»,кафедра полупроводниковой электроники, ул. Бандеры, 12, 79013 Львов, Украина*

Рассмотрены процессы рассеяния электронов на различных точечных дефектах решетки нитрида галлия со структурой сфалерита. Во всех расчетах принимается во внимание принцип близкодействия. Элементы матрицы перехода были оценены с использованием самосогласованных волновой функции и потенциала, полученных в рамках теории функционала электронной плотности из первых принципов. Такой подход позволяет избежать использования параметров подгонки для шести механизмов рассеяния электронов. Рассчитаны температурные зависимости подвижности электронов в диапазоне 30-300 K. Результаты, полученные с помощью близкодействующих моделей рассеяния, лучше согласуются с экспериментом, чем в случае использования дальнодействующих моделей. Впервые получены свойства переноса электронов с использованием близкодействующих моделей, в основе которых лежат рассчитанные из первых принципов с помощью проекционных присоединенных волн самосогласованные собственные функции и потенциалы.

**Ключевые слова**: Электронный транспорт. Точечные дефекты. DFT расчет.

## Розсіяння електронів на близькодіючому потенціалі точкових дефектів в GaN зі структурою сфалерит: розрахунок з перших принципів

О.П. Малик, С.В. Сиротюк

*Національний університет «Львівська політехніка», кафедра напівпровідникової електроніки, вул.Бандери, 12, 79013 Львів, Україна*

Розглядаються процеси розсіяння електронів на різних точкових дефектах гратки в нітриду галію зі структурою сфалериту. У всіх розрахунках береться до уваги принцип близькодії. Елементи матриці переходу були оцінені з використанням самоузгоджених хвильової функції і потенціалу, отриманих в рамках теорії функціонала електронної густини з перших принципів. Такий підхід дозволяє уникнути використання підгінних параметрів для шести механізмів розсіювання електронів. Розраховано температурні залежності рухливості електронів в діапазоні 30-300 K. Результати, отримані за допомогою близькодіючих моделей розсіяння краще узгоджуються з експериментом, ніж у випадку використання далекодіючих моделей. Вперше отримані властивості переносу електронів з використанням близькодіючих моделей, в основі яких лежать розраховані з перших принципів за допомогою проекційних приєднаних хвиль самоузгоджені власні функції і потенціали кристала

**Ключові слова:** Електронний транспорт. Точкові дефекти. DFT розрахунок.

### СПИСОК ЛІТЕРАТУРИ

1. O.P. Malyk, *Mater. Sci. Engineer. B* **129**, 161 (2006).
2. O.P. Malyk, *J. Nano- Electron. Phys.* **8**, No2, 02018 (2016).
3. X. Gonze, B. Amadon, P.-M. Anglade, J.-M. Beuken, F. Bottin, P. Boulanger, F. Bruneval, D. Caliste, R. Caracas, M. Cote, T. Deutsch, L. Genovese, Ph. Ghosez, M. Giantomassi, S. Goedecker, D.R. Hamann, P. Hermet, F. Jollet, G. Jomard, S. Leroux, M. Mancini, S. Mazevet, M.J.T. Oliveira, G. Onida, Y. Pouillon, T. Rangel, G.-M. Rignanese, D. Sangalli, R. Shaltaf, M. Torrent, M.J. Verstraete, G. Zerah, J.W. Zwanziger, *Comput. Phys. Commun.* **180**, 2582 (2009).
4. P.E. Blöchl, C. Först, J. Schimpl, *Bull. Mater. Sci.* **26**, 33 (2003)
5. N.A.W. Holzwarth, A.R. Tackett, G.E. Matthews, *Comp. Phys. Comm.* **135**, 329 (2001).
6. A.R. Tackett, N.A.W. Holzwarth, G.E. Matthews, *Comp. Phys. Comm.* **135**, 348 (2001).
7. J. P. Perdew, A. Ruzsinszky, G.I. Csonka, O.A. Vydrov, G.E. Scuseria, L. A. Constantin, X. Zhou, K. Burke, *Phys. Rev. Lett.* **100**, 136406 (2008).
8. J.P. Perdew, L.A. Konstantin, E. Sagvolden, K. Burke, *Phys. Rev. Lett.* **97**, 223002 (2006).
9. X. Gonze, F. Jollet, F. Abreu Araujo, D. Adams, B. Amadon, T. Applencourt, C. Audouze, J.-M. Beuken, J. Bieder, A. Bokhanchuk, E. Bousquet, F. Bruneval, D. Caliste, M. Cote, F. Dahm, F. Da Pieve, M. Delaveau, M. Di Gennaro, B. Dorado, C. Espejo, G. Geneste, L. Genovese, A. Gerossier, M. Giantomassi, Y. Gillet, D.R. Hamann, L. He, G. Jomard, J. Laflamme Janssen, S. Le Roux, A. Levitt, A. Lherbier, F. Liu, I. Lukačević, A. Martin, C. Martins, M.J.T. Oliveira, S. Ponce, Y. Pouillon, T. Rangel, G.-M. Rignanese, A.H. Romero, B. Rousseau, O. Rubel, A.A. Shukri, M. Stankovski, M. Torrent, M.J. Van Setten, B. Van Troeye, M.J. Verstraete, D. Waroquiers, J. Wiktor, B. Xu, A. Zhou, J.W. Zwanziger, *Comp. Phys. Comm.* **205**, 106 (2016).
10. H.J. Monkhorst, J.D. Pack, *Phys. Rev. B* **13**, 5188 (1976).
11. C. de Boor, *A Practical Guide to Splines* (Springer-Verlag: New York: 1978).
12. J.G. Kim, A.C. Frenkel, H. Liu, R.M. Park, *Appl. Phys. Lett.* **65**, 911(1994).
13. I. Vurgaftman, J.R. Meyer, L.R. Ram-Mohan, *J. Appl. Phys.* **89**, 5815 (2001).
14. G. Ramirez-Flores, H. Navarro-Contreras, A. Lastras-Martinez, R.C. Powell, J.E. Greene, *Phys. Rev. B* **50**, 8433 (1994).
15. J. Petalas, S. Logothetidis, S. Boultadakis, M. Alouani, J.M. Wills. *Phys. Rev. B* **52**, 8082 (1995).
16. S.K. Pugh, D.J. Dugdale, S. Brand, R.A. Abram, *Semicond. Sci. Technol.* **14**, 23 (1999).
17. A.T. Meney, E.P. O'Reilly, A.R. Adams, *Semicond. Sci. Technol.* **11**, 897 (1996).
18. V.W.L. Chin, T.L. Tansley, T. Osotchan, *J. Appl. Phys.* **75**, 7365 (1994).
19. H. Harima, *J. Phys. Condens. Mat.* **14**, R967 (2002).
20. H. Siegle, L. Eckey, A. Hoffmann, C. Thomsen, B.K. Meyer, D. Schikora, M. Hankeln, K. Lischka, *Solid State Commun.* **96**, 943 (1995).
21. A.F. Wright. *J. Appl. Phys.* **82**, 2833 (1997).
22. M.S. Shur, B. Gelmont, A. Khan, *J. Electron. Mater.* **25**, 777 (1996).
23. O.P. Malyk, *J. Alloy. Compd.* **371**, 146 (2004).